

Received October 18, 2020, accepted November 9, 2020, date of publication November 26, 2020, date of current version December 10, 2020.

Digital Object Identifier 10.1109/ACCESS.2020.3040744

Color Laser Marking: Repeatability, Stability and Resistance Against Mechanical, Chemical and Environmental Effects

HAMID ROOZBAHANI¹, (Member, IEEE), MARJAN ALIZADEH¹, HEIKKI HANDROOS¹, (Member, IEEE), AND ANTTI SALMINEN²

¹Lappeenranta-Lahti University of Technology, 53851 Lappeenranta, Finland

²University of Turku, 20014 Turku, Finland

Corresponding author: Hamid Roozbahani (hamid.roozbahani@lut.fi)

This work was supported in part by APPOLO funded by EU FP7-ICT under Grant 609355, and in part by the Finnish Strategic Research Council under Grant 313349 /313397.

ABSTRACT In this paper, utilizing the technology of color laser marking of stainless steel in industrial productions is investigated from the perspective of repeatability and stability of produced color markings. The color laser marking has remarkable advantages over conventional metal coloring methods; however, in order to implement this technology in industry, the reliability, stability and quality of resulting markings must be endorsed. For this purpose, an AISI 304 color palette made up of fifteen colors was evolved. The dependence of produced colors on different laser processing parameters were analyzed. Afterward, the produced colors were tested utilizing optical, scanning electron and atomic force microscopy, and the configuration of oxide films was specified through Raman spectroscopy. The obtained colors had proper uniformity, brightness, and cover almost all spectral regions. Also, color standardization and palette repeatability test were performed by assessing and evaluating the reflectance spectra of the formed colors. The color palette demonstrated high repeatability for all colors except for one specific color. Moreover, the stability of color markings in terms of environmental, mechanical and chemical resistance was investigated. The resulting colors showed high resistance in most of the environmental conditions; however, exposure to very high temperatures and extreme humidity (100°C, 90%) and low temperature and extreme humidity (−40°C, 90%) leads to deterioration of few colors. Color marks showed high hardness and excellent mechanical stability to external impacts and outstanding resistance to various chemicals, excluding acidic solutions and salts.

INDEX TERMS Color laser marking, color marking stability, environmental resistance, laser oxidation, mechanical/chemical resistance, wear resistance.

I. INTRODUCTION

Product marking is an essential part of the production cycle, which provides the necessary information about the product and serves as a marketing tool to draw consumers' attention to a specific product. Although various types of marks are applied to products, permanent markings are more desired. Different techniques, including indenting, electrochemical etching, engraving, dot peen, and laser marking, can be utilized to create permanent marking. Nowadays, laser marking is extensively utilized in various sections of the production line for a variety of applications to create high-resolution

The associate editor coordinating the review of this manuscript and approving it for publication was Guijun Li¹.

everlasting marks. The laser marking method is efficient, non-contact, and applies to both metallic and nonmetallic types of surfaces. Furthermore, it does not require extra supplements or solvents and does not produce waste; thus, it is environmentally sustainable. Moreover, surface coloring by laser is possible using color laser marking technology, which is the focus of this paper. Color laser marking has been known for a long time, so, many researches have been conducted about using different kinds of laser sources, effects of environmental conditions on the results and analysis of physical and chemical properties of the surfaces before and after laser treatment. A laser marking technique for substrates such as ceramic, glass, plastic, and metal was proposed by Axtell III *et al.* [1]. Li *et al.* obtained a comprehensive

perception of the process of oxide-forming during interaction of UV laser beam with stainless steel in the air [2]. Modeling of coloring on stainless steel surfaces with color pixels through surface heating using laser was conducted by Lehmuskero *et al.* [3]. Dusser *et al.* demonstrated attaining material modifications utilizing ultra-fast laser pulses via producing polarization-dependent structures, which can create particular color designs [4]. Color laser marking technology for metal coloring was also studied by Gorny *et al.* [5]. Veiko *et al.* studied metal surface coloration method, where small-scale periodic structures formed with nanosecond laser pulses [6]. Liu *et al.* investigated the recent developments in laser technologies for surface coloring and three specific physics mechanisms in the color generation, which are thin film effect of the surface oxidation, laser-induced periodic surface structures (LIPSSs), and laser-induced nanoparticles and nanostructures [7].

In color laser marking technology, reaching the heat of the material to a certain temperature produces a slim oxide film on the metal surface, which is observable because of light interference reflecting from the oxide coating. Different colors can be formed depending on the thickness of the film and by manipulating the laser process parameters such as heating temperature and pulse duration [8]. This technology is used in various oxidizable metals such as titanium, brass, copper and different alloy steel types. While different kinds of lasers like UV, CO₂, or solid-state types can be employed for coloring and marking purposes, pulsed fiber laser is the most favored one, which has prominent advantages over common metal coloring techniques and other laser technologies. Due to high flexibility of the processing parameters, these lasers can be applied in a production line simply. They are economical compared to lasers of ultrashort pulses, convenient to use, and provide laser beam with high quality and stability with short pulse duration [9].

Fiber lasers are transforming various traditional processes in the industry, ranging from cutting, welding, and scribing to marking [10]–[12]. Rapid development of fiber lasers continues to gain market share in material processing applications [13]. Modern manufacturers are interested in using fiber laser technology as a credible technique for making marks on their products. There are numerous researches regarding utilizing fiber lasers for coloring purposes [14]–[17]. Growing interference oxide films on the surface of stainless steel 304L were demonstrated by Adams *et al.* [14]. Analyzing the properties of the created oxide film was addressed by Lawrence *et al.* [15] and Amara *et al.* [16]. The influence of the gas environment on the composition and color of the modified surface by the nanosecond laser is demonstrated by Luo *et al.* [17]. However, some subjects require further investigations to convince the industry to apply color laser marking technology in a wide range. For instance, repeatability, reliability, and sustainability of the colored marks should fulfill the requirements of industrial applications when utilizing this technology. It is crucial to ensure that the marks with the same quality can be generated in serial production

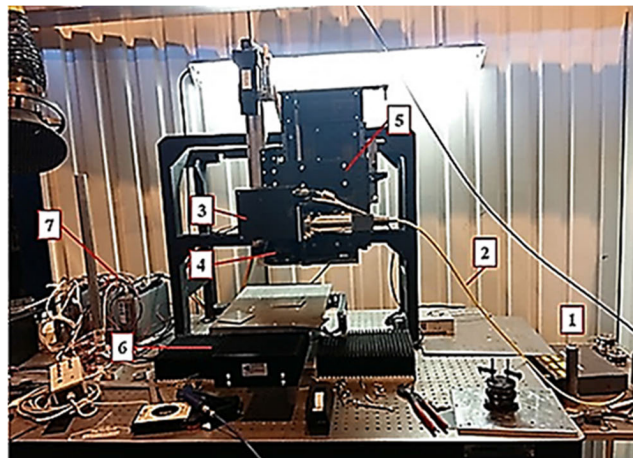


FIGURE 1. Laser marking system based on nanosecond fiber laser.

and be stable under different environmental, mechanical, and chemical conditions. The aim of this paper is to investigate the execution of color laser marking technology in the industry and the limitations of its usage. The reliance of colors produced on the various laser processing parameters is demonstrated and the properties of obtained structures are analyzed. Also, the repeatability of the color palette is confirmed by measuring the reflectance spectra of all colors. Moreover, the hardness of the colored metal structures obtained using color laser marking technology and their resistance to different environmental conditions and chemical solutions is examined.

II. MATERIALS AND METHODS

A. LASER PROCESSING SETUP AND PARAMETERS

Stainless steel contains chromium in its composition, which provides chemical stability and great heat resistance for alloy and makes it suitable for utilization in the laser process. In this study, 2 mm thick plates stainless steel AISI 304 are utilized with the initial roughness level $R_z = 8.42 \mu\text{m}$, reflectance $R(\lambda = 1.06 \mu\text{m}) = 0.75$, thermal diffusivity $a = 3 \times 10^{-6} \text{ m}^2/\text{s}$, thermal conductivity $k = 37 \text{ W/mK}$, melting point = 1800 °C, and boiling point = 3145 °C. At the initial stage, surfaces were cleaned with acetone to avoid any pollution or spot. Ytterbium fiber laser with nanosecond pulses supplied by IPG Photonics Corporation was selected as the source of laser radiation with wavelength $1055 < \lambda < 1075 \text{ nm}$ that generate pulses of duration $4 < \tau < 200 \text{ ns}$ at repetition rate $1.6 < f < 1000 \text{ kHz}$. The setup of the laser processing system, which has been developed for scribing and marking purposes, is presented in Fig. 1, which consists of 1) IPG Photonics nanosecond fiber laser, 2) optical fiber transferring, 3) SCANLAB scan system, 4) lens 100 mm, 5) Neff-Wiesel linear actuator for vertical movement, 6) XY coordinate stage, 7) Kollmorgen ACD servo drives.

Fiber pulsed ytterbium laser radiated and was fed into a collimating system through an optical fiber to form a parallel beam output. A dual-axis galvanometer scanning system

(hurrySCAN II 14 digital scan head from SCANLAB corp.) was installed to move along the X and Y axes. A focusing lens with a focal length of 100 mm was used to focus the laser radiation on the surface of the steel plate. Extra horizontal movements and vertical movements can be performed using a multiaxial linear motor coordinate stage, which allows extending the workspace up to 250 × 250 mm. Laser radiation parameters and scanning speed can be changed using the developed LabVIEW code. Also, any vertical and horizontal movements can be managed through the same code.

A focused laser beam with diameter d_0 , which moves at velocity V_{sc} and pulse repetition rate f irradiates a sample surface line-by-line (Fig. 2). When one scan line is completed with the overlap, the laser beam proceeds along the Y-axis on the next line with overlap $L_y(\%)$ $L_y(\%)$ characterized by hatch distance H .

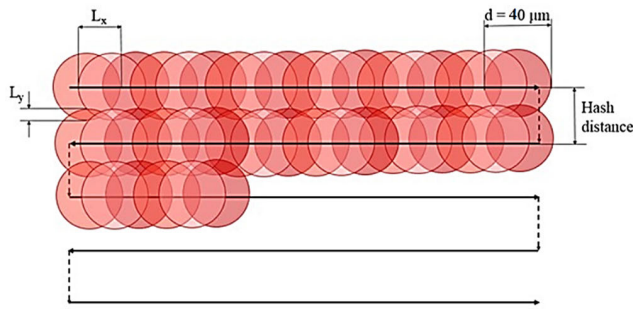


FIGURE 2. Scheme of laser scanning.

Regulating laser processing parameters that control the heat input and distribution on the material can produce various thicknesses. Temperature T on the surface can be calculated by estimating the heat equation solution as Eq. 1 [18]:

$$T(N_x) = \frac{2.I.(1 - R).\sqrt{a}}{k.\sqrt{\pi}} \sum_{n=0}^{N_x} \left[\sqrt{t(N_x) - \frac{n}{f}} - \sqrt{t(N_x) - \left(\frac{n}{f} + \tau\right)} \right] + T_0 \quad (1)$$

where R is the reflectivity on wavelength $1.06 \mu\text{m}$, I is the density of radiation power, k is the material thermal conductivity, a is the material thermal diffusivity, f is the repetition rate, T_0 is the initial sample temperature, τ is the pulse duration. N_x, N_y , which are the number of pulses per spot with diameter d_0 along the X and Y axis, determine the effective time of action according to Eq. 2 [18].

$$t_{eff_x,y} = N_x N_y \tau = \frac{d_0^2 \tau f N}{V_{SC}} \quad (2)$$

Therefore, N_x and N_y can be calculated by Eq. 3 and 4, respectively.

$$N_x = \frac{d_0 f}{V_{SC}} \quad (3)$$

$$N_y = \frac{d_0}{H} \quad (4)$$

Since N_x and N_y include all parameters required for laser processing, it is appropriate to use them together with the power density I_0 formulated as Eq. 5 to define the different regimes.

$$I_0 = \frac{4P}{\pi d_0^2} \quad (5)$$

where P is laser power, and d_0 is the spot diameter. Laser beam diameter is required to calculate the power density of laser radiation. In this study, the laser beam diameter used is $40 \mu\text{m}$.

B. SPECTRA PROPERTIES

Ocean Optics CHEM4-VIS-NIR USB4000 spectrophotometer was employed to measure the reflectance spectra of the material under study before and after laser exposure. A halogen lamp of 15 V with the filament dimensions of $360 \times 2000 \text{ nm}$ served as the illumination source. Light delivers into the illumination device integrated into the probe tool via optical fiber. Illumination and probe fibers have $200 \mu\text{m}$ diameter. To achieve the accurate movements of samples within the workstation up to size $150 \times 150 \text{ mm}$, STANDA two-axis coordinate table is used.

C. COLOR NOTATION AND CALCULATIONS

In order to determine the calorimetric parameters of the material surface, the relative spectral distribution of reflection coefficient $\beta(\lambda)$ is used according to Eq. 6 [19]:

$$\beta(\lambda) = \frac{\Phi_{ob}(\lambda)}{\Phi_s(\lambda)} \quad (6)$$

where $\Phi_{ob}(\lambda)$ is the relative spectral distribution of the light source radiant flux reflected from the object surface; $\Phi_s(\lambda)$ is the spectral distribution of the radiant flux of the light source reflected from the white reference surface. Hence, the object's colorimetric parameters are specified by the spectral distribution of the radiant flux of the light source $S(\lambda)$, the relative spectral distribution of the reflection coefficient $\beta(\lambda)$, and the color matching functions of the CIE XYZ system ($x(\lambda), y(\lambda)$ and $z(\lambda)$). The color coordinates X, Y, Z, can be defined in Eq. 7-9 [19]:

$$X = k \int_{\lambda=360}^{\lambda=830} S(\lambda) \beta(\lambda) \bar{x}(\lambda) d\lambda \quad (7)$$

$$Y = k \int_{\lambda=360}^{\lambda=830} S(\lambda) \beta(\lambda) \bar{y}(\lambda) d\lambda \quad (8)$$

$$Z = k \int_{\lambda=360}^{\lambda=830} S(\lambda) \beta(\lambda) \bar{z}(\lambda) d\lambda \quad (9)$$

where k is the normalizing factor, calculated by the Eq. 10.

$$k = 100 / \int_{\lambda=360}^{\lambda=830} S(\lambda) \bar{y}(\lambda) d\lambda \quad (10)$$

The color coordinates X, Y, Z calculated above can be transformed into any color coordinate system like the CIE RGB system.

D. SURFACE TOPOLOGY ANALYSIS

In this study, Carl Zeiss Axio Imager A1M optical microscope is used to analyze the samples on a microscale. The microscope is equipped with lenses with different magnification in the power range of $20\times$ - $100\times$. Scanning electron microscope (SEM) JEOL JSM 7001F with a resolution of approximately $1\ \mu\text{m}$ was used to examine the treated surface more closely. Veeco Dimension 3100 in contact mode was employed to determine three-dimensional topology atomic force microscopy (AFM) of the obtained area. The 16-bit resolution on all three axes can be achieved utilizing a NanoScope IIIa controller and Quadrex signal processor.

E. ENVIRONMENTAL CHAMBER TESTING

Thermotron SM-3200 Benchtop Environmental Chamber was used to examine the colors in exposure to various environmental conditions. The temperature range of the chamber is from -40 to $130\ ^\circ\text{C}$, and the humidity range is from 20% to 95% RH.

F. HARDNESS TESTING

Microhardness tester PMT-3M from LOMO with an extensive load range 0.0196 to 4,9 N was used to examine the hardness of samples. The tester is equipped with a microscope with possible magnification to $130\times$, $500\times$, and $800\times$, which allows measuring even very small indents.

III. DEVELOPMENT OF COLOR PALETTE

The color laser marking process involves melting and solidification of the material in sequence, which leads to oxidation and nitridation on the material surface. The final surface and the formation of the oxide film is the outcome of multiple pulsed laser operation, which varies according to the laser heat and overlap value of laser pulses. The result of the relief and color of the surface is affected by almost all laser source parameters. In this study the dependency of obtained colors on the scanning speed, laser power, pulse duration and frequency of laser pulses is investigated. Investigating the obtained color dependency on surface relief is not the target of this study. In the first stage, the dependency of colors on laser power density versus scan speed is assessed with frequency $f = 60\ \text{kHz}$, pulse duration $\tau = 100\ \text{ns}$, hatch distance $H = 0.01\ \text{mm}$, and varying laser power density I_0 from $8 \cdot 10^7$ to $1.6 \cdot 10^8\ \text{W/cm}^2$ with the step of $0.8 \cdot 10^7\ \text{W/cm}^2$ and varying scanning speed V_{sc} from 300 to 750 mm/s with 50 mm/s step. The result is shown in Fig. 3.

The result reveals that as the power increases, the colors do not change significantly, and only the parametric window moved to higher scanning speed values for each color. Considering that greater productivity can be obtained at higher intensities, the color dependency on the scanning speed with available maximum constant power 20 W was investigated in the next phase with the same frequency, hatch distance, and pulse duration parameters. Scanning speed was first altered from 450 to 850 mm/s with 10 mm/s step, and next changed

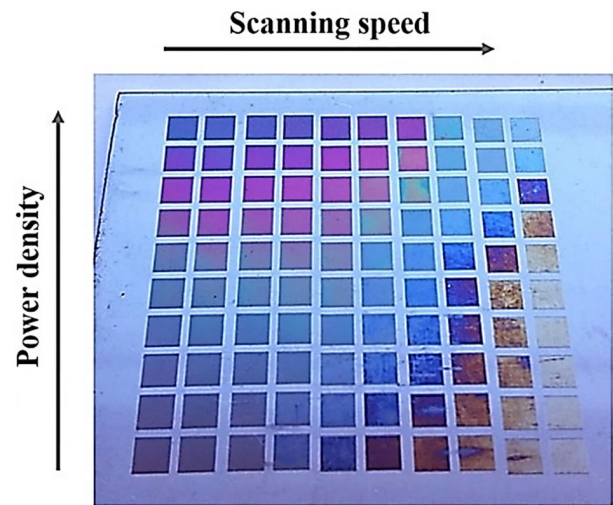


FIGURE 3. The dependency of produced color on the power densities vs scanning speed ($I_0 = 8 \cdot 10^7 - 1.6 \cdot 10^8\ \text{W/cm}^2$, $V_{sc} = 300\text{-}750\ \text{mm/s}$, $f = 60\ \text{kHz}$, $\tau = 100\ \text{ns}$, $H = 0.01\ \text{mm}$).

from 50 to 150 mm/s with the same step. The results are presented in Fig. 4.



FIGURE 4. The dependency of produced color on the scanning speed ($I_0 = 1.6 \cdot 10^8\ \text{W/cm}^2$, $f = 60\ \text{kHz}$, $\tau = 100\ \text{ns}$, $H = 0.01\ \text{mm}$, $V_{sc} = 450\text{-}850\ \text{mm/s}$: line 1 to 4 and $V_{sc} = 50\text{-}150\ \text{mm/s}$: line 5 from left to right).

As shown in Fig. 4, in low scanning speed, only dark gray colors emerge, while as the scanning speed increases colors vary in this sequence: dark green, dark violet, wine red, orange, light green, gold and light blue.

To investigate the dependency of colors to the frequency of laser pulses, the experiment was performed with $I_0 = 1.6 \cdot 10^8\ \text{W/cm}^2$, $\tau = 100\ \text{ns}$, $H = 0.01\ \text{mm}$, $V_{sc} = 450\text{-}1200\ \text{mm/s}$ with 50 mm/s step and varying frequency which was changed from up to down for every two lines as 100, 200, 500 and 1000 kHz, correspondingly. Fig. 5 demonstrates color dependency on scanning speed for various frequencies.

The test result revealed that specific colors such as light pink, aquamarine, or bright purple might be obtained with higher frequency regimes. At $f = 1000\ \text{kHz}$ just silver colors are formed for the entire range of scanning speed; hence, the parametric color window could not be produced in the mentioned frequency, although it can be utilized in final palette for producing white or silver color due to its fast-producing speed.

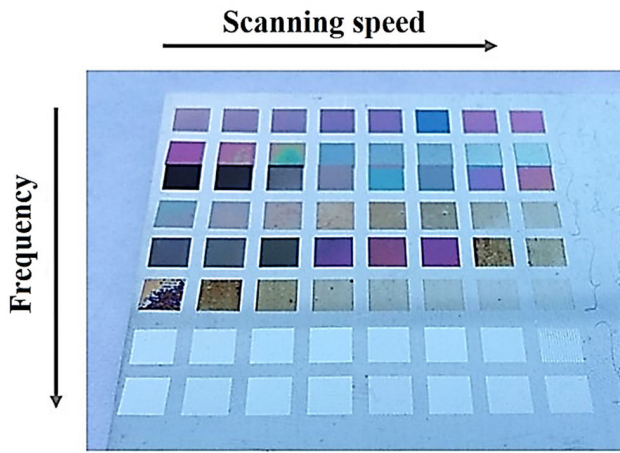


FIGURE 5. The dependency of produced color on the scanning speed for various frequencies ($I_0 = 1.6 \cdot 10^8 \text{ W/cm}^2$, $\tau = 100 \text{ ns}$, $H=0.01 \text{ mm}$, $V_{sc} = 450\text{-}1200 \text{ mm/s}$, $f=100 \text{ kHz}$: lines No 1,2; $f= 200 \text{ kHz}$: lines No 3,4; $f=500 \text{ kHz}$: lines No 5,6; $f=1000 \text{ kHz}$: lines No 7,8.

The experiment for investigating the dependency of colors to pulse duration was conducted with two different power densities $I_0 = 0.8 \cdot 10^7$ and $I_0 = 1.6 \cdot 10^7 \text{ W/cm}^2$ and two different pulse durations $\tau = 4$ and $\tau = 8 \text{ ns}$ with scanning speed $V_{sc} = 50\text{-}200 \text{ mm/s}$ with 10 mm/s step and $HH = 0.01 \text{ mm}$. The result of the test is displayed in Fig. 6.

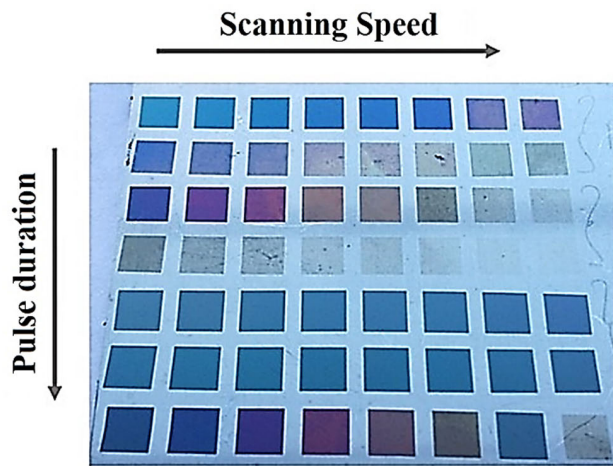


FIGURE 6. The dependency of produced color on the scanning speed for the various pulse durations ($V_{sc} = 50\text{-}200 \text{ mm/s}$, $H=0.01 \text{ mm}$, $f=60 \text{ kHz}$, lines No 1,2: $\tau = 4 \text{ ns}$, $I_0 = 0.8 \cdot 10^8 \text{ W/cm}^2$; lines No 3,4: $\tau = 4 \text{ ns}$, $I_0 = 1.6 \cdot 10^8 \text{ W/cm}^2$; lines No 5,6: $\tau = 8 \text{ ns}$, $I_0 = 0.8 \cdot 10^7 \text{ W/cm}^2$; line No 7: $\tau = 8 \text{ ns}$, $I_0 = 1.6 \cdot 10^8 \text{ W/cm}^2$).

As seen from Fig. 6, the pulse duration has a significant effect on the color. The color sequence, shades and roughness of the surface under the color are different for shorter and longer pulse durations. For longer pulse durations ($\tau \gg 20 \text{ ns}$), visually colors are vitreous, and the underneath material is smoother compared to pulses with shorter pulse durations. In contrast, with shorter pulses the parametric window transfers to scanning speed with lower values, which reduces

TABLE 1. Processing parameters of the final color palette.

Number	N_x	N_y	$I_0, 10^8 \text{ W/cm}^2$
1	13	4	0.8
2	7	4	1.6
3	44	4	1.6
4	11	4	1.6
5	10	4	1.6
6	44	4	1.6
7	57	4	1.6
8	8	4	1.6
9	7	4	1.6
10	4	4	1.6
11	4	4	1.2
12	3	4	1.2
13	22	4	1.6
14	200	4	1.6
15	24	4	1.6

marking efficiency. Almost the same color dependence is observed for pulse durations 4 ns and 8 ns ; however, for pulse duration 8 ns scanning speed is higher and obtained colors are more consistent. Based on the performed analysis, the number of pulses per spot (N_x, N_y) and power density (I_0), were selected to develop the color palette with fifteen different shades for stainless steel AISI 304 as shown in Table 1.

The visual display of obtained color palette is presented in Fig. 7.

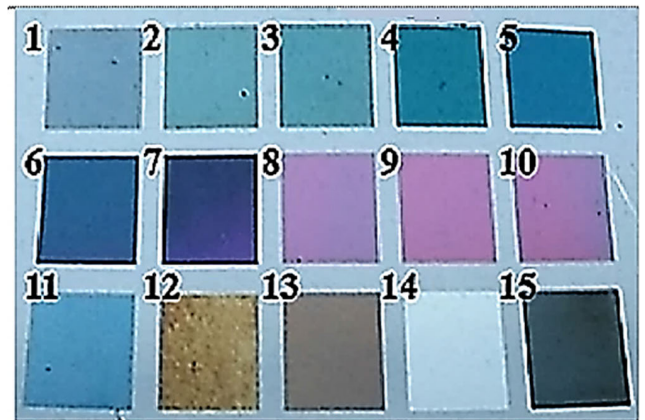


FIGURE 7. Ultimate color palette obtained for AISI 304 stainless steel.

1) ANALYSIS OF OBTAINED STRUCTURES

Optical microscopy was used to view the microstructure of developed colors and to analyze the oxide film structure of the color palette. Micro images of each produced color and the untreated surface are shown in Fig. 8.

Assessing the micro images reveals that the created color samples with wide overlaps, i.e., great N_x and N_y values, are composed of separate regions of diverse colors. Moreover, the oxide film structure will be different depending on the overlapping and laser processing regime. Some samples, including samples no. 8-10, 15 have firmly marked bar microstructure while samples no. 11, 12, 14 have irregular

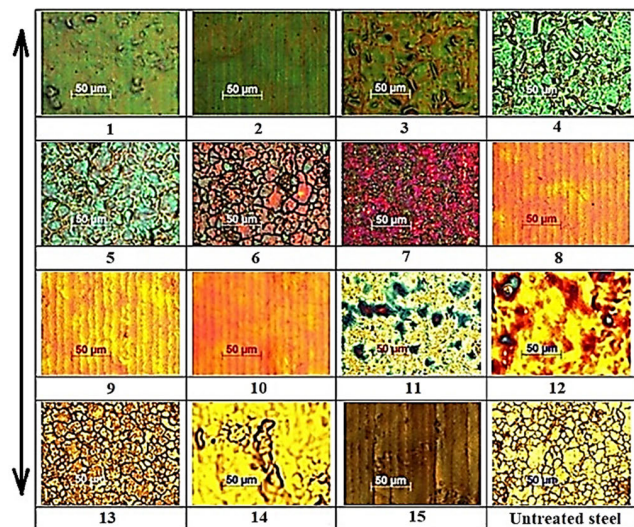


FIGURE 8. Micro images of the color palette for stainless steel AISI 304.

microstructure, and samples no. 6 and 7 have a grained-like structure. To examine the structures in more detail, scanning electron microscopy (SEM) images from some samples were taken with 5kV electron beam accelerating voltage (Fig. 9).

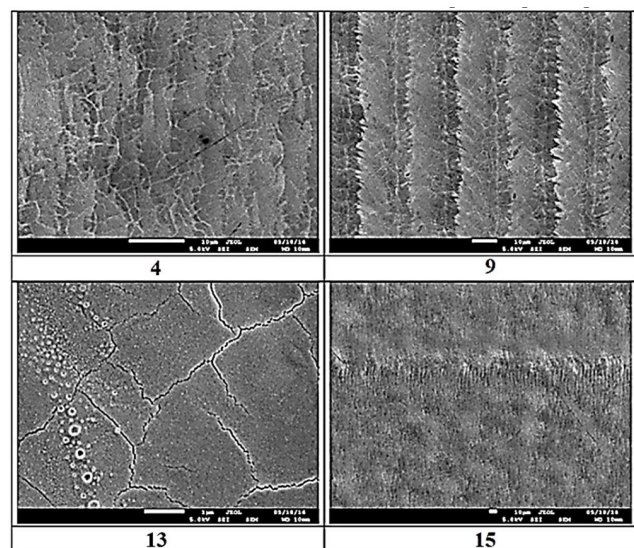


FIGURE 9. SEM images of the samples.

The structures were also examined by atomic force microscopy (AFM) operating in contact mode. Sample no. 9 surface profile and 3D plane are displayed in Fig. 10.

In fact, the sample has periodically repetitive relief that is corresponding to the scan geometry. The maximum and average roughness height are almost 2.6 and 1.5 μm , respectively, which are quite short compared to the roughness of the material surface ($R_z = 8.42 \mu\text{m}$).

To determine the chemical composition of obtained samples, Raman scattering spectra method was used in this study [16]. Solid-state laser was employed for Raman scattering

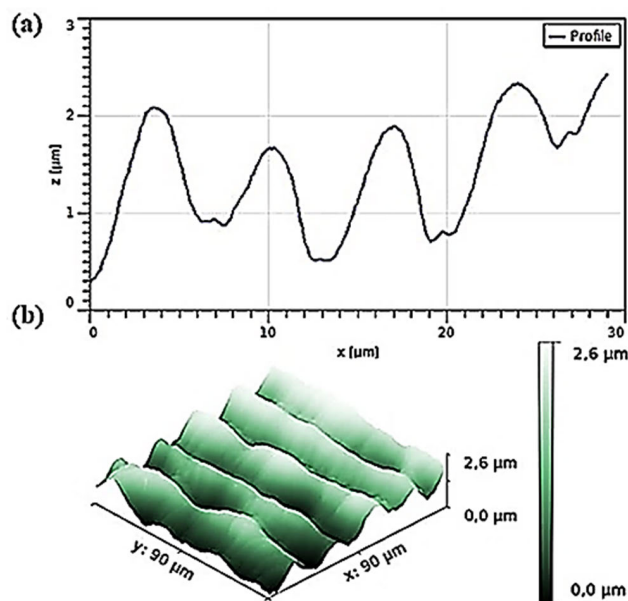


FIGURE 10. AFM analysis of sample no. 9: (a)profile (b)3D plane.

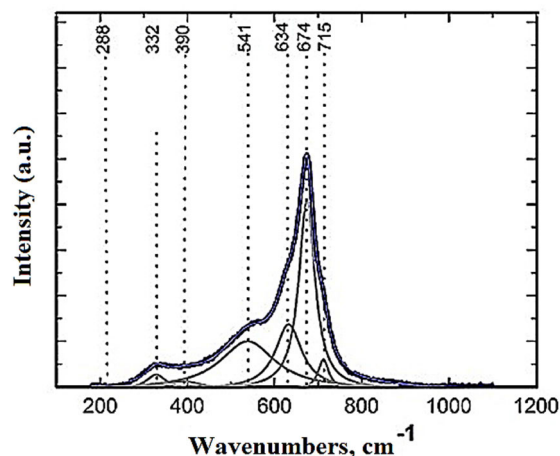


FIGURE 11. The Raman spectra of the sample No. 9.

analysis. It initiates scattering of the sample no. 9 surface with 532 nm wavelength and 1 mW output power (Fig. 11). Lorentz fitting function was applied to the graph to precisely characterize the position of the peaks. Seven Lorentzian peaks at 288, 332, 390, 541, 634, 674 and 715 cm^{-1} were specified. FeCr_2O_4 has the own phonon modes, which matches properly with 541, 634, 674 cm^{-1} [20]; hence, it means the presence of FeCr_2O_4 in the films produced. Peaks at 288, 332, 390 and 715 cm^{-1} are related to the existence of maghemite (Fe_2O_3) or the maghemite-rich region that can exist because of the oxide film in addition to untreated steel [21].

IV. REPEATABILITY AND WEAR RESISTANCE TEST OF LASER COLORED SURFACE

The coating quality is vital in industrial production and should meet the requirements of standard organizations, manufacturers, and consumers. The produced colors explained

in section 3 were examined for repeatability and stability in terms of environmental, mechanical, and chemical resistance.

A. REPEATABILITY OF OBTAINED COLORS

Repeatability is a crucial factor in color coatings in a sense that the same color can be reproducible in different production cycles. Color determination is carried out by reflection and transmission spectra analysis of objects. In this research work, the standard CIE RGB coordinate space is used to control sample colors, in which red (R), green (G), and blue (B) flux components form the coordinates [22]. The additive rule in Eq. 11 is used to define colors in this system [23].

$$C = r\bar{R} + g\bar{G} + b\bar{B} \tag{11}$$

where R^- , G^- , B^- are the units of relevant primary colors and r, g, b are the number of units of each primary colors required to build the particular color C . Relative color coordinates can be calculated similarly as in the CIE XYZ system by Eq. 12-14 [23].

$$r = r/(r + g + b) \tag{12}$$

$$g = g/(r + g + b) \tag{13}$$

$$b = b/(r + g + b) \tag{14}$$

The reflectance spectra of each color are required to calculate the color coordinates. As illustrated in Fig. 12, each colored square is divided into 25 regions; hence, the ultimate spectrum is the mean spectra of the chosen areas (Fig. 13).

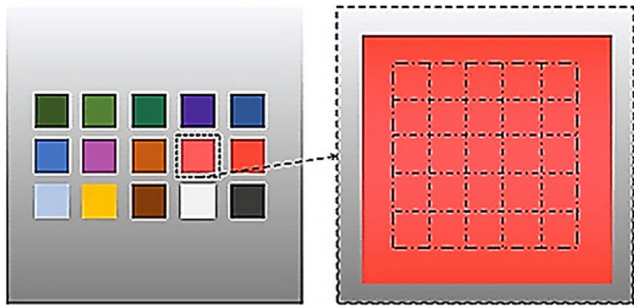


FIGURE 12. Color measurement scheme.

Depending on the type of peaks that appear in the wavelength, four groups of spectra can be identified. The first group (Fig. 13a) is plane spectra that do not have any obvious peaks in the wavelength range and their original appearance looks like spectra of untreated steel. In the second group (Fig. 13b), one clear peak occurs between 500 to 700 nm. Two peaks happen about 420 and 550 nm correspondingly in the third group (Fig. 13c). In the last group (Fig. 13d), peaks are expanded compared to the prior group. It is speculated that the interference impact in denser oxide film and surface coloration cause peaks appearance. A program was developed in LabVIEW to calculate the color coordinates in CIE RGB space for each sample. The result of the calculations is demonstrated in Table 2.

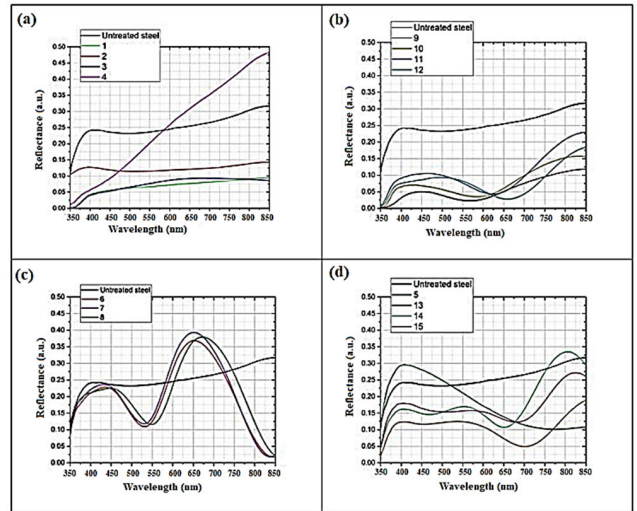


FIGURE 13. Produced colors reflectance spectra.

TABLE 2. Calculated color coordinates in CIE RGB space of the final palette.

Number	Color coordinates		
	R	G	B
1	84	92	89
2	49	71	45
3	123	157	121
4	81	136	101
5	98	140	133
6	111	110	149
7	175	132	174
8	173	59	83
9	159	68	59
10	169	74	96
11	132	135	164
12	206	189	78
13	166	155	118
14	224	227	226
15	65	75	72

Twenty color palettes were made in order to examine the repeatability, six of which are shown in Fig. 14.

The color difference of palettes determines the repeatability of colors produced by applied laser technology. The International Commission on Lighting set the standard for color differences using the Delta E concept definition, which is the change assessment in visual perception of two certain colors. In this study concept of delta E has been utilized to evaluate the color difference [24], [25]. For the color repeatability purpose, delta E = 2 is typically utilized [24]. The average of the delta E value was calculated using MATLAB code for all the samples of the same color which are presented in Fig. 15.

According to Fig. 15 the repeatability of all colors is satisfactory, which qualifies them to be employed in the production line. The majority of color squares (no. 1, 2, 3, 7, 8, 14, 15) have superb delta E, so that the color variation is not perceivable even through close observation by an experienced observer. Samples no. 4, 6, 10, and 11 have acceptable delta

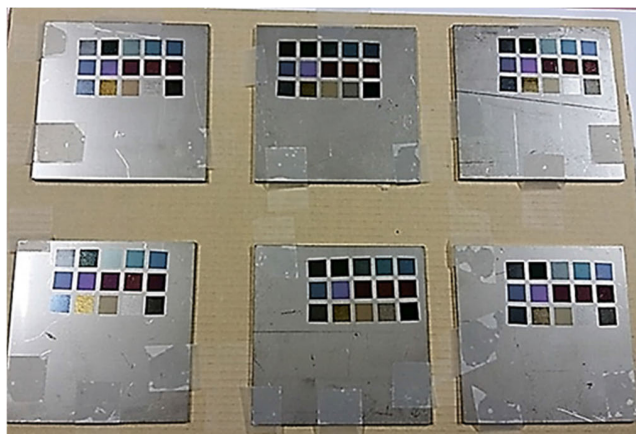


FIGURE 14. Six identical color palettes produced with the equal laser processing parameters.

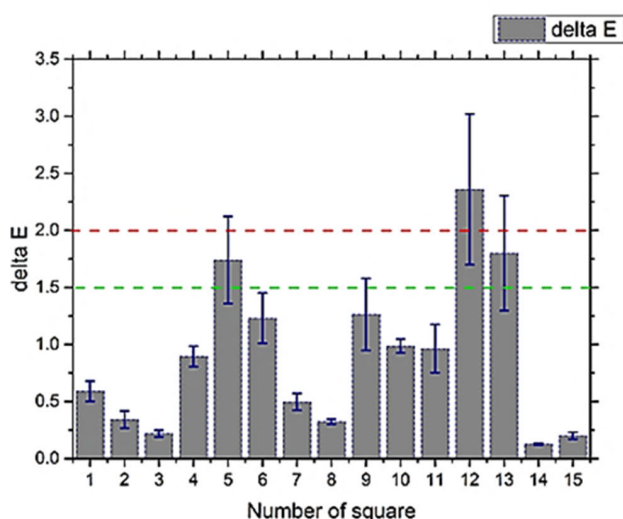


FIGURE 15. Delta E values of fifteen different colors averaged for ten samples. Green line is the minimal delta E value which is perceptible by the human eye. Red line is the maximum delta E value acceptable in production.

E values in a sense that color difference can be detected just by experienced observer in proper lighting conditions. Square no. 9 still has a satisfactory delta E value that is acceptable for use in production. Squares no. 5 and 13 have upper average delta E values, which can be associated with angle effect [26], although these colors can still be inserted in the color palette as visually, no differences were identified between the samples. Square no. 12 has the greatest delta E value (2.36) and accordingly lowest repeatability, which means an ordinary observer can perceive the difference. Therefore, this color cannot be recommended for further usage. This problem may be solved by regulating the laser processing parameters or selecting different regimes that can provide alike color.

B. ENVIRONMENTAL CHAMBER TEST

The coatings and marks of the products must withstand various environmental conditions and must not alter in the

period of product use. In this research, environmental test chamber was performed based on four different operational conditions. Regularly, the experiments are conducted with the temperature and humidity conditions not actually expected, such as a combination of extremely low or high temperatures (−40, −20, 40, 100 °C) with high humidity (70%, 90%). In this way, the stability of samples under normal conditions is ensured; and also, the short duration of test exposure (24 hours) compared to the actual operation time is compensated. The first test was performed for the environmental condition of temperature −20 °C and humidity 70%. The result shows no change in colors or materials after 24 hours in the environmental test chamber, as displayed in Fig. 16. No damages or defects were found in the oxide films using optical microscopy analyses.

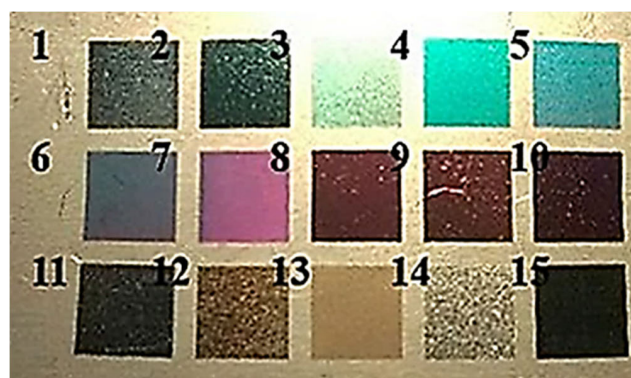


FIGURE 16. Color palette after 24hr exposure in the environmental test chamber at temperature −20 °C and humidity 70 %.

The second test was performed for the environmental condition of temperature −40 °C and humidity 90%. The result reveals multiple minor surface variations after 24 hours of exposure to the environmental chamber, as illustrated in Fig. 17.



FIGURE 17. Color palette after 24hr of exposure in the environmental test chamber at temperature - 40 °C and humidity 90%.

Pictures of the problematic areas and micro images of faults are shown in Fig. 18a and Fig. 18b, respectively. One

murky spot with a diameter of about $400\ \mu\text{m}$ appeared on the surface of square no. 1 (Fig. 18a left). Upon detailed observation under an optical microscope, it was found that the stain is an amended oxide layer with remarkable damage (Fig. 18b left). However, the remaining part of the square does not indicate any alteration. The presence of the spot is probably due to the existence of some dirt on the surface or impurity in the material. The creation of these types of defects has a random characteristic and has appeared only once during the entire test. In square no. 5, color slightly varied from blue to gray on the edge of the area under treatment, which might be caused due to the partial oxidation of the sample (Fig. 18a middle). Under the microscope (Fig. 18b middle), only one damaged area measuring approximately $1 \times 1.5\ \text{mm}$ was showed. As these types of faults were characteristic of a single color, it can be concluded that it is probably related to the laser operation regime. In square no. 10, color has changed from wine red to yellow in the approximate $1 \times 0.5\ \text{mm}$ area (Fig. 18a right). The microscopic analysis represents the spoiled region where the oxide film has been etched while the structure was not demolished (Fig. 18b right). This kind of defect can be caused by high humidity, which is likely to enlarge with increasing test exposure time.

It can be concluded that, in general, laser colored marks can withstand the environmental condition with low temperatures and high humidity. However, for these purposes, it is recommended that the color palette be slightly amended.

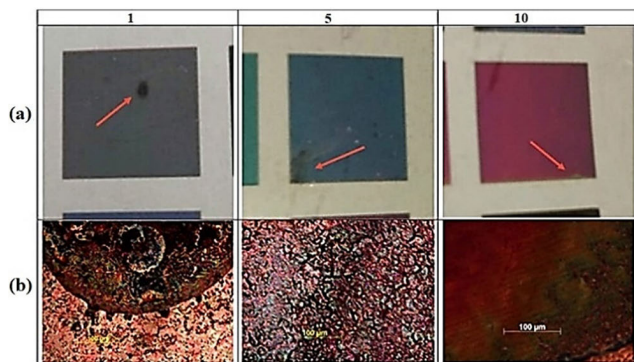


FIGURE 18. Color faults after 24hr exposure in the environmental test chamber at temperature $-40\ ^\circ\text{C}$ and humidity 90%: a) pictures b) micro images.

The third test was performed with the environmental condition of temperature $40\ ^\circ\text{C}$ and humidity 70%. Results showed that the palette does not have a significant fault and no change in color or metal surface has been observed after 24 hours in the environmental test chamber, as displayed in Fig. 19.

Nevertheless, after careful inspection, a stain with an approximate size of $1 \times 2\ \text{mm}$ was detected on one corner of square no. 4, only visible at a certain angle, as shown in Fig. 20a. Microscope analysis shows that the observed spot is the darkening of part of the oxide film, which might be caused due to the adjustments of laser processing parameters



FIGURE 19. Color palette after 24hr exposure in the environmental test chamber at temperature $40\ ^\circ\text{C}$ and humidity 70%.

(Fig. 20b). Generally, the color palette is relatively stable in the environmental condition of test 3.

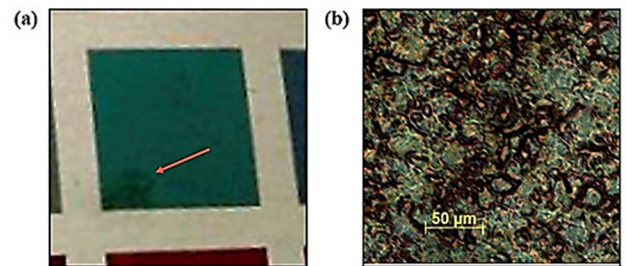


FIGURE 20. Color fault of square no. 4 after 24hr exposure in the environmental test chamber at temperature $40\ ^\circ\text{C}$ and humidity 70%: (a) pictures (b) micro image.

The last test was conducted for extremely rough environmental conditions of temperature $100\ ^\circ\text{C}$ and humidity 90%. The result showed some stains and dark spots on the metal surface itself and on the colors, which are visible in Fig. 21.

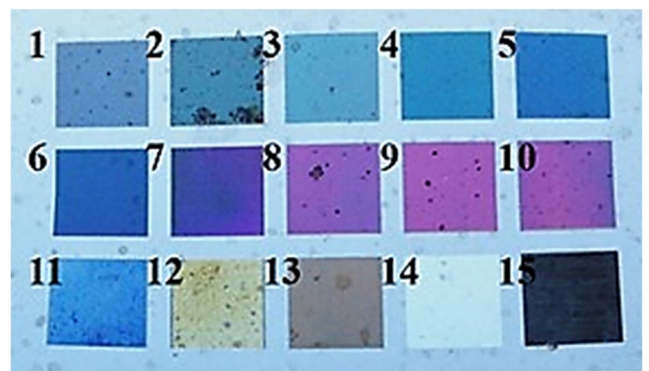


FIGURE 21. Color palette after 24hr exposure in the environmental test chamber at temperature $100\ ^\circ\text{C}$ and humidity 90%.

The majority of evident faults are presented in Fig. 22a left and middle. Almost entire colored squares no. 2 and 8 were

damaged in the form of dark stains with sizes from 500 μm up to 3 mm, which are independent of the laser processing parameters. Optical microscopic analysis in Fig. 22b left and Fig. 22b middle implies that the appeared spots are the entire demolition of the oxide film caused most likely due to the evaporation of the condensed water on the surface because of the humidity/temperature condition of the test chamber. Besides, the untreated surface demonstrates poor resistance to such types of environmental conditions (Fig. 22a right). When the surface was viewed with an optical microscope, dark spots with dimensions of 0.5 to 2 mm were found on the entire untreated steel surface (Fig. 22b right). Darkening may be related to the rusting of particular surface regions caused by condensation and subsequent evaporation of water on the metal, leading to partial oxidation.

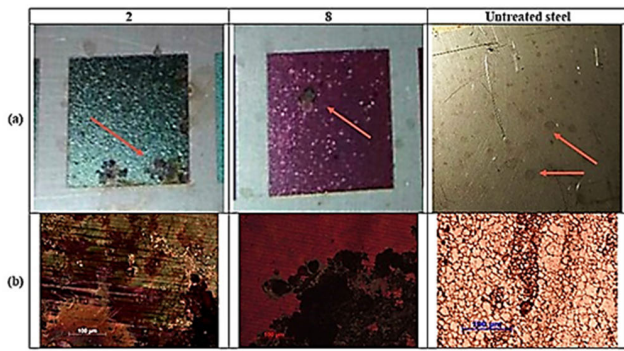


FIGURE 22. Color faults after 24hr exposure in the environmental test chamber at temperature 100 °C and humidity 90%: a) pictures b) micro images.

Therefore, the test experiment results reveal that the color laser marking is not proper to apply for harsh environmental conditions with very high temperature and humidity. However, if the adequate circulation of air in the operating place is available, the risk of damage to the colored area can be remarkably reduced.

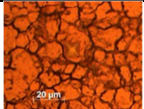
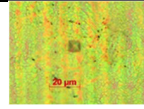
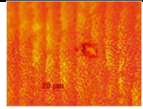
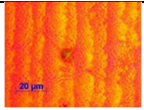
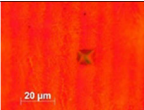
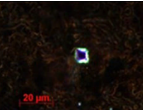
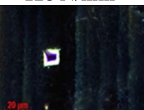
C. MECHANICAL RESISTANCE TEST

Mechanical resistance of a material can be determined via various techniques, including Vickers, Brinell, Knoop, Rockwell tests, etc. [27]. Vickers microhardness test was conducted in this study to evaluate the mechanical resistance of the untreated material and produced samples. According to the Vickers test method, hardness can be calculated by Eq. 15 [27].

$$H = 0.189 \frac{F}{d^2} \tag{15}$$

where F is the force of normal load and d is the length of the diagonals left by the indenter. Four measurements were performed for each sample. The Vickers microhardness values measured for each sample, the dispersion of the obtained results on average values, and micro images of indent are presented in Table 3.

TABLE 3. Microhardness of produced samples.

<p>Untreated steel Hardness 1=186 N/mm² Deviation 1=6 N/mm² Hardness 2=171 N/mm² Deviation 2=9 N/mm² Hardness 3=190 N/mm² Deviation 3=10 N/mm² Hardness 4=173 N/mm² Deviation 4=7 N/mm² Hardness mean = 180 N/mm²</p> 	<p>Sample no. 2 Hardness 1=139 N/mm² Deviation 1=3N/mm² Hardness 2=144 N/mm² Deviation 2=8 N/mm² Hardness 3=129 N/mm² Deviation 3=7N/mm² Hardness 4=132 N/mm² Deviation 4=4 N/mm² Hardness mean = 136 N/mm²</p> 	<p>Sample no. 8 Hardness 1=141 N/mm² Deviation 1=8N/mm² Hardness 2=127 N/mm² Deviation 2=6 N/mm² Hardness 3=138 N/mm² Deviation 3=5N/mm² Hardness 4=126 N/mm² Deviation 4=7 N/mm² Hardness mean = 133 N/mm²</p> 
<p>Sample no. 9 Hardness 1=136 N/mm² Deviation 1=7 N/mm² Hardness 2=119N/mm² Deviation 2=10 N/mm² Hardness 3=124 N/mm² Deviation 3=5N/mm² Hardness 4=137 N/mm² Deviation 4=8 N/mm² Hardness mean = 129 N/mm²</p> 	<p>Sample no. 10 Hardness 1=143N/mm² Deviation 1=8N/mm² Hardness 2=139N/mm² Deviation 2=4 N/mm² Hardness 3=132 N/mm² Deviation 3=3N/mm² Hardness 4=126 N/mm² Deviation 4=9 N/mm² Hardness mean = 135 N/mm²</p> 	<p>Sample no. 11 Hardness 1=175 N/mm² Deviation 1=8N/mm² Hardness 2=164 N/mm² Deviation 2=3 N/mm² Hardness 3=171 N/mm² Deviation 3=4N/mm² Hardness 4=158 N/mm² Deviation 4=9 N/mm² Hardness mean = 167 N/mm²</p> 
<p>Sample no. 15 Hardness 1=131 N/mm² Deviation 1=3N/mm² Hardness 2=135 N/mm² Deviation 2=7 N/mm² Hardness 3=126 N/mm² Deviation 3=2N/mm² Hardness 4=120 N/mm² Deviation 4=8 N/mm² Hardness mean = 128 N/mm²</p> 		

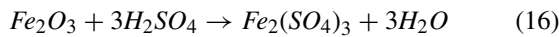
The highest hardness belongs to sample no. 11, which is probably due to the relatively small overlap and lower power density than other colors that leads to forming thinner oxide film during laser processing. The substrate may play a significant role in the hardness measurement of thick films. Nonetheless, the surface hardness of produced samples is relatively high compared with the mechanical hardness of untreated steel (180 N/mm²), as indicated by Table 3, that can endorse the coating resistance against external mechanical influence.

D. CHEMICAL RESISTANCE TEST

Products may be exposed to various chemical agents in different operating locations; hence it is vital to evaluate the resistance of marks and coatings of the products against chemical solutions. In this study, chemical resistance of color laser markings against most common chemical compounds

i.e., sulfuric acid, sodium hydroxide, ethanol, surfactant, and sodium chloride, are examined.

Sulfuric acid is used in different fields of industry, such as pulp and paper, agriculture, metals and water treatment. Although AISI 304 is resistant to various corrosive environments, its sensitivity to sulfuric environments was a crucial reason to examine the resistance of produced samples by color laser markings on AISI 304 against sulfuric acid. Low concentration 3% was chosen for the initial test, which was planned to be increased in case of obtaining satisfactory resistance results. The first test was carried out with 3% sulfuric acid solution for 48 hours. Colors got less saturated after 24 hours and all colors were completely or partially removed from the surface and some colors were changed to another color. The test result is shown in Fig. 23. The chemical process in sulfuric acid occurs according to the reaction shown in Eq. 16:



As $Fe_2(SO_4)_3$ is incredibly soluble in water, no extra products from the chemical reaction remained. Therefore, it can be concluded that produced color markings cannot interact with an acidic environment.

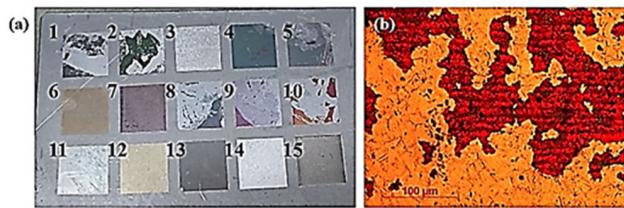


FIGURE 23. Color palette after 48hr in 3% sulfuric acid: (a) picture (b) micro image of square no. 9 as a sample.

The second test was performed for 10% solution of NaOH for 48 hours. No significant changes in colors were observed after 24 hours or 48 hours. The test result is shown in Fig. 24. With attention to the fact that NaOH solutions, which are used for manufacturing purposes usually have 3-5% concentration, it leads to the conclusion that obtained color coating is relatively stable in an alkaline environment. Examples for such manufacturing applications are acid neutralization, PH regulations, bleaching, degreasing, cleaning, etherification and esterification, etc.

The third test was performed with technical ethanol 98% for 48 hours. Colors did not change, and no faults were observed in the visual and microscopic analysis, as displayed in Fig. 25.

The subsequent experiment was performed with standard industrial surfactant (New ultrasil 69), which has PH 13 and 1.5% phosphorus, for 48 hours. Surfactant is the main component of many practical applications like soaps, cosmetics, emulsions, anti-fogs, detergents, etc. The test result showed that colors did not change, and no faults were noticed, as displayed in Fig. 26.

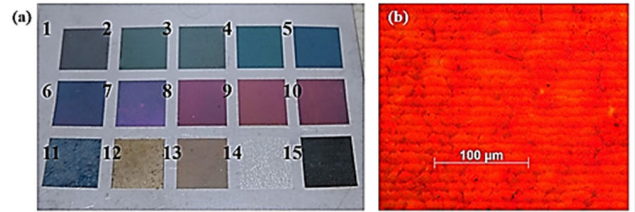


FIGURE 24. Color palette after 48hr in 10% NaOH: (a) picture (b) micro image of square no. 9 as a sample.

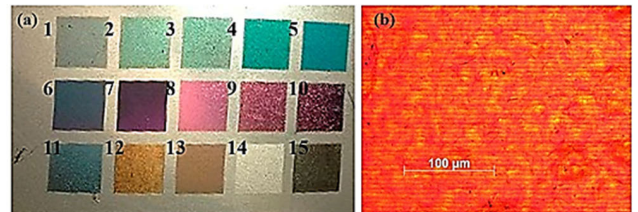


FIGURE 25. Color palette after 48hr in 98% ethanol: (a) picture (b) micro image of square no. 9 as a sample.

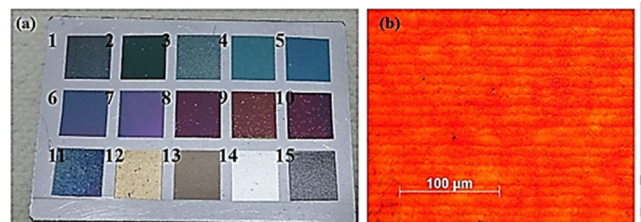


FIGURE 26. Color palette after 48hr in Ultrasil New 69 surfactant: (a) picture (b) micro image of square no. 9.

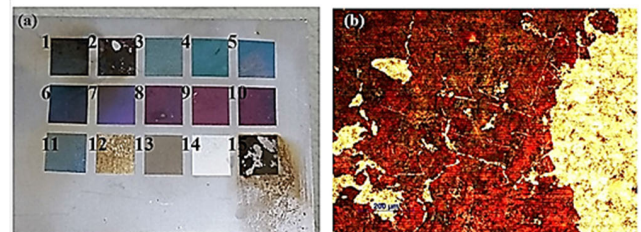


FIGURE 27. Color palette after 24hr in 10% NaCl: (a) picture (b) micro image of square no. 2.

The last experiment was performed with NaCl 10% water solution for 24 hours. The experiment results showed that only some colors could resist against the saline solution, and most of them have been damaged. The most damage was detected in samples no. 1, 2 and 15. Furthermore, the entire palette sample began to rust, starting from the edge of each square extending to the untreated substance. On squares no. 2 and 15, the oxide film separated partially and removed from the surface. The test result is shown in Fig. 27.

V. CONCLUSION

Surface laser color marking attracts a lot of attention both in scientific and industrial communities due to the capability

of producing high-quality marks consisting of several colors in the same production cycle without using any additional dyes or chemicals. In the presented paper, the potential of utilizing color laser marking technology in industrial production is discussed in detail. The properties of the obtained coatings are tested to ensure repeatability of colors and wear resistance to mechanical, chemical and environmental conditions.

The laser processing system, developed for the purposes of this research work, is based on nanosecond ytterbium fiber laser on a multi-axial platform for the workpiece and the possibility of vertical movement of the laser scan head. In the preliminary phase, the scanning system was calibrated and the specifications of the laser beam in focal point were determined. In order to find the appropriate value of power density, the distribution of the laser spot on the surface was measured. The dependency of the colors produced on laser processing parameters including scanning speed, pulse duration, radiation power and pulse repetition rate was investigated. Twenty color palettes of stainless steel AISI 304 was developed based on the performed analysis. Each sample consists of 15 squares of different colors with a dimension of 8×8 mm. The produced oxide films were examined using optical microscopy and scanning electron microscope (SEM). Also, surface topology was performed using atomic force microscopy (AFM). In order to assess the structure of the oxide films obtained, Raman scattering spectroscopy was carried out. Peak analysis revealed that four types of oxide compositions have been created accordant with laser processing parameters. The film consists of two main components: Fe_2O_3 and FeCr_2O_4 , which are in accordance with the data previously obtained by other researchers. The standardization of colors was performed based on the standard of the International Commission on Illumination. The light coordinates in the CIE RGB color space were calculated and reflection spectra were obtained from each color with the help of spectrophotometric measurements. Results ascertain that created colors have proper consistency, brightness and cover roughly all spectral regions. Repeatability of the obtained colors has been proved by calculating the delta E value. In general, the color palette verifies outstanding repeatability, although it is recommended that one particular color to be replaced because it does not meet the minimum requirement of delta E value for industrial applications. Stability of color laser marking in diverse environmental conditions was investigated using a climatic test chamber for four different operational conditions, including low and high temperatures and high humidity. The results demonstrated that the color palette has a great resistance in most environmental conditions; however, at excessively high temperature and high humidity (100°C, 90%), limited destroy has created in some colors, and also the untreated metal surface was damaged. Also, prolonged exposure to temperature -40°C and humidity 90% leads to an insignificant alteration of multiple colors, which were required to be exchanged by more stable ones. The mechanical stability of the color palette was evaluated by determining the Vickers hardness value before and after applying laser

treatment by employing a microhardness tester equipped with a diamond pyramid. After treatment, the hardness of most of the samples is in average 26% less than the hardness of the substrate material, which still confirms high hardness of the coatings and consequently ensures the mechanical resistance of color markings against external impacts. Moreover, with attention to the fact that the color is not obtained by adding an extra coating layer but by altering the material surface itself, the cohesion of these labels is much higher than the color markings created by conventional methods. Stability of the color palette versus different chemical compounds, including sulfuric acid, sodium hydroxide, ethanol, surfactant, and sodium chloride, was examined. It was proved that the produced laser color markings are resistant to chemicals like caustic soda, surfactant and alcohol. On the other hand, prolonged interaction with acidic solutions and salts can damage color marks. Therefore, the interaction of color laser marks with environments with the presence of acidic and salty components should be avoided.

The results of this paper have an impressive contribution to implementing color laser marking technology in the industry. Directions for future research would be the development of stainless steel AISI 304 color palette to include at least 30 different colors and increasing productivity of marking by using stronger lasers and higher frequency modes. Applying the technology for diverse oxidizable metals, including titanium, brass, chromium, tungsten, different grades of steel and developing color palettes and parametric windows for each material would be another future research direction.

REFERENCES

- [1] E. A. Axtell, III, D. C. Kapp, T. A. Knell, M. Novotny, and G. E. Sakoske, "Laser marking method and apparatus," U.S. Patent 6238847, May 29, 2001. [Online]. Available: <https://patents.google.com/patent/US6238847B1/en>
- [2] Z. L. Li, H. Y. Zheng, K. M. Teh, Y. C. Liu, G. C. Lim, H. L. Seng, and N. L. Yakovlev, "Analysis of oxide formation induced by UV laser coloration of stainless steel," *Appl. Surf. Sci.*, vol. 256, no. 5, pp. 1582–1588, Dec. 2009, doi: [10.1016/j.apsusc.2009.09.025](https://doi.org/10.1016/j.apsusc.2009.09.025).
- [3] A. M. Lehmuskero, V. Kontturi, J. Hiltunen, and M. Kuittinen, "Modeling of laser-colored stainless steel surfaces by color pixels," *Appl. Phys. B, Lasers Opt.*, vol. 98, pp. 497–500, Sep. 2009, doi: [10.1007/s00340-009-3734-2](https://doi.org/10.1007/s00340-009-3734-2).
- [4] B. Dusser, Z. Sagan, H. Soder, N. Faure, J. P. Colombier, M. Jourlin, and E. Audouard, "Controlled nanostructures formation by ultra fast laser pulses for color marking," *Opt. Exp.*, vol. 18, no. 3, pp. 2913–2924, 2010, doi: [10.1364/OE.18.002913](https://doi.org/10.1364/OE.18.002913).
- [5] S. G. Gorny, V. P. Veiko, G. Odintsova, E. Gorbunova, A. Loginov, and Y. Karlagina, "Color laser marking of metals," *Photonika*, vol. 6, pp. 34–44, Jan. 2013.
- [6] V. Veiko, Y. Karlagina, M. Moskvina, V. Mikhailovskii, G. Odintsova, P. Olshin, D. Pankin, V. Romanov, and R. Yatsuk, "Metal surface coloration by oxide periodic structures formed with nanosecond laser pulses," *Opt. Lasers Eng.*, vol. 96, pp. 63–67, Sep. 2017, doi: [10.1016/j.optlaseng.2017.04.014](https://doi.org/10.1016/j.optlaseng.2017.04.014).
- [7] H. Liu, W. Lin, and M. Hong, "Surface coloring by laser irradiation of solid substrates," *APL Photon.*, vol. 4, no. 5, May 2019, Art. no. 051101, doi: [10.1063/1.5089778](https://doi.org/10.1063/1.5089778).
- [8] V. Veiko, G. Odintsova, E. Gorbunova, E. Ageev, A. Shimko, Y. Karlagina, and Y. Andreeva, "Development of complete color palette based on spectrophotometric measurements of steel oxidation results for enhancement of color laser marking technology," *Mater. Des.*, vol. 89, pp. 684–688, Jan. 2016, doi: [10.1016/j.matdes.2015.10.030](https://doi.org/10.1016/j.matdes.2015.10.030).

- [9] F. Brihmat-Hamadi, E. H. Amara, and H. Kellou, "Characterization of titanium oxide layers formation produced by nanosecond laser coloration," *Metall. Mater. Trans. B*, vol. 48, no. 3, pp. 1439–1449, Mar. 2017, doi: [10.1007/s11663-017-0952-6](https://doi.org/10.1007/s11663-017-0952-6).
- [10] W. Shi, A. Schulzgen, R. Amezcuca, X. Zhu, and S.-U. Alam, "Fiber lasers and their applications: Introduction," *J. Opt. Soc. Amer. B, Opt. Phys.*, vol. 34, no. 3, p. FLA1, Mar. 2017, doi: [10.1364/JOSAB.34.00FLA1](https://doi.org/10.1364/JOSAB.34.00FLA1).
- [11] H. Roozbahani, P. Marttinen, and A. Salminen, "Real-time monitoring of laser scribing process of CIGS solar panels utilizing high-speed camera," *IEEE Photon. Technol. Lett.*, vol. 30, no. 20, pp. 1741–1744, Oct. 15, 2018, doi: [10.1109/LPT.2018.2867274](https://doi.org/10.1109/LPT.2018.2867274).
- [12] S. McCulloch, A. Hassey, and P. Harrison, "Fiber laser performance in industrial applications," *Proc. SPIE*, vol. 8603, Feb. 2013, Art. no. 86030C, doi: [10.1117/12.2004838](https://doi.org/10.1117/12.2004838).
- [13] B. Shiner, "Fiber lasers continue to gain market share in material processing applications," *Manuf. Eng.*, vol. 156, pp. 79–85, Feb. 2016.
- [14] D. P. Adams, V. C. Hodges, D. A. Hirschfeld, M. A. Rodriguez, J. P. McDonald, and P. G. Kotula, "Nanosecond pulsed laser irradiation of stainless steel 304L: Oxide growth and effects on underlying metal," *Surf. Coatings Technol.*, vol. 222, pp. 1–8, May 2013, doi: [10.1016/j.surfcoat.2012.12.044](https://doi.org/10.1016/j.surfcoat.2012.12.044).
- [15] S. K. Lawrence, D. P. Adams, D. F. Bahr, and N. R. Moody, "Mechanical and electromechanical behavior of oxide coatings grown on stainless steel 304L by nanosecond pulsed laser irradiation," *Surf. Coatings Technol.*, vol. 235, pp. 860–866, Nov. 2013, doi: [10.1016/j.surfcoat.2013.09.013](https://doi.org/10.1016/j.surfcoat.2013.09.013).
- [16] E. H. Amara, F. Haïd, and A. Noukaz, "Experimental investigations on fiber laser color marking of steels," *Appl. Surf. Sci.*, vol. 351, pp. 1–12, Oct. 2015, doi: [10.1016/j.apsusc.2015.05.095](https://doi.org/10.1016/j.apsusc.2015.05.095).
- [17] F. Luo, W. Ong, Y. Guan, F. Li, S. Sun, G. C. Lim, and M. Hong, "Study of micro/nanostructures formed by a nanosecond laser in gaseous environments for stainless steel surface coloring," *Appl. Surf. Sci.*, vol. 328, pp. 405–409, Feb. 2015, doi: [10.1016/j.apsusc.2014.12.053](https://doi.org/10.1016/j.apsusc.2014.12.053).
- [18] V. P. Veiko, G. Odintsova, E. Ageev, Y. Karlagina, A. Loginov, A. Skuratova, and E. Gorbunova, "Controlled oxide films formation by nanosecond laser pulses for color marking," *Opt. Exp.*, vol. 22, no. 20, pp. 24342–24347, 2014, doi: [10.1364/OE.22.024342](https://doi.org/10.1364/OE.22.024342).
- [19] P. Artal, *Handbook of Visual Optics, Two-Volume Set*, 1st ed. Boca Raton, FL, USA: CRC Press, 2017.
- [20] D. J. Gardiner, C. J. Littleton, K. M. Thomas, and K. N. Strafford, "Distribution and characterization of high temperature air corrosion products on iron-chromium alloys by Raman microscopy," *Oxidation Met.*, vol. 27, nos. 1–2, pp. 57–72, Feb. 1987, doi: [10.1007/BF00656729](https://doi.org/10.1007/BF00656729).
- [21] R. J. Thibreau, C. W. Brown, and R. H. Heidersbach, "Raman spectra of possible corrosion products of iron," *Appl. Spectrosc.*, vol. 32, no. 6, pp. 532–535, Nov. 1978. [Online]. Available: <http://as.osa.org/abstract.cfm?URI=as-32-6-532>.
- [22] A. Sharma, *Understanding Color Management*, 1st ed. Clifton Park, NY, USA: Thomson/Delmar Learning, 2004.
- [23] J.J. Koenderink, *Color for the Sciences*, 1st ed. Cambridge, MA, USA: MIT Press, 2010.
- [24] (2020). *Datacolor. Color Differences Tolerances*. Accessed: Oct. 1, 2020. [Online]. Available: <http://industrial.datacolor.com/support/articles/>
- [25] G. Sharma, W. Wu, and E. N. Dalal, "The CIEDE2000 color-difference formula: Implementation notes, supplementary test data, and mathematical observations," *Color Res. Appl.*, vol. 30, no. 1, pp. 21–30, Feb. 2005, doi: [10.1002/col.20070](https://doi.org/10.1002/col.20070).
- [26] E. I. Ageev, Y. M. Andreeva, P. N. Brunkov, Y. Y. Karlagina, G. V. Odintsova, D. V. Pankin, S. I. Pavlov, V. V. Romanov, and R. M. Yatsuk, "Influence of light incident angle on reflectance spectra of metals processed by color laser marking technology," *Opt. Quantum Electron.*, vol. 49, no. 2, Jan. 2017, doi: [10.1007/s11082-016-0876-4](https://doi.org/10.1007/s11082-016-0876-4).
- [27] G. Revankar, "Introduction to hardness testing," in *Mechanical Testing and Evaluation*, H. Kuhun and D. Medlin, Eds. Cleveland, OH, USA: ASM International, 2000, pp. 197–202.



HAMID ROOZBAHANI (Member, IEEE) received the D.Sc.Tech. and Master of Science degrees in mechatronics from the Lappeenranta-Lahti University of Technology (LUT). Since 1999, he has been working as a project manager in several projects. He is currently working as a Research Scientist, a Project Manager, and a Lecturer with LUT. He is also a Project Manager of EU funded project APPOLO and TIERA - LUT Mobile Robot Project.



MARJAN ALIZADEH received the B.Sc. degree in electrical engineering – control from the Ferdowsi University of Mashhad, Iran, in 2003, and the M.Sc. degree in electrical engineering – industrial electronics from the Lappeenranta-Lahti University of Technology, Finland, in 2017. From 2003 to 2015, she was working in electrical engineering in industry. She is currently working as a Project Researcher with the Lappeenranta-Lahti University of Technology.



HEIKKI HANDROOS (Member, IEEE) received the D.Sc. (Tech.) degree from the Tampere University of Technology. Since 1992, he has been a Professor of machine automation with the Lappeenranta-Lahti University of Technology. He has been a Visiting Professor with the University of Minnesota, Peter the Great St. Petersburg Polytechnic University, and the National Defense Academy, Japan. He has published about 250 international scientific articles and supervised around 20 D.Sc. theses. He has held several positions of trust in the American Society of Mechanical Engineers. He has led several important domestic and international research projects. His research interests include modeling, design and control of mechatronic transmissions to robotics, and virtual engineering.



ANTTI SALMINEN received the D.Sc. degree. He is currently a Professor of mechanical engineering with the University of Turku. He is also a Docent in manufacturing technology with LUT University. He has more than 30 years of experience of laser-based manufacturing processes and welding in both academia and industry. He has been a Principal Investigator in several research projects funded by national, Nordic, and European funding agents. He has published more 100 peer-reviewed scientific and more than 150 scientific conference publications. His research interests include process and laser system development, product design utilizing laser processing and additive manufacturing, and monitoring of thermal processes especially for welding and additive manufacturing. He has supervised ten Ph.D., 70 master, and 16 bachelor theses. He is also supervising eight Ph.D. theses. He is a Member of Board of the Finnish Association for additive manufacturing and a Deputy Member of Board of the Finnish Welding Society and a National Delegate in IIW commissions I, IV, and X.

• • •